Int. J. Electrochem. Sci., 12 **(2017)** 6653 – 6661, doi: 10.20964/2017.07.46

International Journal of ELECTROCHEMICAL SCIENCE
www.electrochemsci.org

Short Communication

Coin-cell Supercapacitors Based on CVD Grown and Vertically Aligned Carbon Nanofibers (VACNFs)

Amin M. Saleem[1, 2,*], *Andrea Boschin*[3], *Du-Hyun Lim*[3], *Vincent Desmaris*[1], *Patrik Johansson*[3], *Peter Enoksson*[2]

[1] Smoltek AB, Regnbågsgatan 3, SE-417 55 Gothenburg, Sweden
[2] Micro and Nanosystems Group, Electronics Materials and Systems Laboratory, Department of Microtechnology and Nanoscience, Chalmers University of Technology, SE-412 96 Gothenburg, Sweden
[3] Department of Physics, Chalmers University of Technology, SE-412 96 Gothenburg, Sweden
[*]Email: amin@smoltek.com

Received: 14 March 2017 / *Accepted:* 29 April 2017 / *Published:* 12 June 2017

Complete supercapacitors (SCs) comprising vertically aligned carbon nanofibers (VACNFs) as electrode materials have been assembled as coin-cells. The VACNFs were grown directly onto the current collector by direct current plasma enhanced chemical vapor deposition (DC-PECVD), thereby providing excellent contact with the current collector, but also eliminating the need of any binder. The vertical alignment facilitates fast ion transport and the electrolyte to access the entire surface of the CNFs. The morphology of the VACNFs was evaluated by scanning electron microscopy (SEM), while the performance was assessed by several methods: cyclic voltammetry (CV), electrochemical impedance spectroscopy (EIS) and device related cycling by galvanostatic charge/discharge. The capacitance, 3.64 mF/cm^2, is >15 times higher than the capacitance of a coin-cell without CNFs and the cyclic performance shows these proof-of-concept SCs to retain >80% of the capacitance after 2000 full charge/discharge cycles. The direct growth of VACNFs as electrodes at the current collector opens pathways for SC production using existing coin-cell battery production technology.

Keywords: VACNF; PECVD; coin-cell; supercapacitor

1. INTRODUCTION

There is a strong trend of exploration of novel energy storage and energy conversion systems with high power and energy densities, much due to the growing large need of portable energy as well as for replacing fossil fuels to reduce environmental pollution. Batteries are renown as energy storage devices due to their high energy density, but suffer from low power density and short cycle life as

compared to capacitors with higher power densities and longer cycle life, but at the cost of low energy density.

The electric double layer capacitor (EDLC) also known as supercapacitor (SC) or ultracapacitor is an energy storage technology based on physisorption and electrostatic accumulation of charges at the electrode surfaces, with a power density larger than for batteries, moderate energy density, as well as faster charge/discharge and longer cycle life (up to 1 million cycles) [1, 2]. SCs have the potential to be employed in heavy machinery and transport to provide high power, in portable electronics for quick charging, and not the least in medical device in human bodies, where changing the device is not only difficult and expensive but also a health hazard.

Carbon based nanomaterials such as graphene [3], carbon nanotubes (CNTs) [4] and carbon nanofibers (CNFs) [5, 6, 7] are widely used as SC electrodes due to their extraordinary electrical and mechanical properties, chemical stability and high surface area. The surface area has a large influence on the SC capacity and it can be further increased by creating pores in the electrode materials [8]. These pores can be of different types; micropores (< 2 nm), mesopores (2-50 nm) and macropores (> 50 nm). The micropores and mesopores contribute significantly to the surface area and high specific capacitance but a significant amount of very small sized micropores are inaccessible to the electrolyte ions – and hence the capacitance is not optimal. Moreover, the binders are often used to attach the electrode materials on the current collector which cause a reduction in the available surface area of the electrode and as they are electrochemically inactive, lower the SC capacity. The coin-cell SCs are made using carbon nanomaterials as electrode, and commercial coin-cell casing which is an existing industry adopted casing for energy storage. The graphene composites based coin-cell SCs have readily been shown to give high gravimetric capacitance 100-271 F/g [9, 10, 11], however, the fabrication involves several process steps which could potentially increase the production cost.

Vertically aligned carbon nanostructures have been explored for energy storage due to the formation of regular pore sizes allowing to maximize the electrode surface area accessible by the electrolyte, and to facilitate fast ion transport, and thereby high capacitance retention at higher charge/discharge current densities [12]. The direct growth of an electrode material onto a current collector enables the metallic contact to reduce the equivalent series resistance (ESR) where ESR is the sum of the bulk electrolyte resistance, the resistance of the active electrode material and the contact resistance between electrode and current collector. As an example, VACNTs grown by chemical vapor deposition (CVD) onto Inconel current collectors have fairly low ESR of 550 mΩ [13]. Similarly, graphene nanowalls directly grown onto stainless steel (SS) current collectors at high temperature (1000 ^{o}C) as electrode materials and 6M KOH as a electrolyte give low ESR of 800 mΩ [1].

VACNFs has drawn significant attention for industrial adaptation and been explored for on-chip microelectronic packaging interconnects, high frequency applications and energy storage, much owing to their outstanding electrical and mechanical properties in combination with a CMOS compliant growth temperature (390 ^{o}C) [14]. The latter has been found to be difficult to achieve with other allotropes of carbon such as CNTs and graphene delaying industrial adaptation [15]. In the present work, we have exploited the electrical and high effective surface area properties of industry compatible VACNFs for fabricating coin-cell SCs. The VACNFs are grown directly onto industrial standard SS current collectors by a two-step process; 1) a quick deposition of catalyst followed by 2)

the growth of CNFs at 550 ^{o}C and finally packaged in a coin-cell assembly to be readily used in electronic devices.

2. EXPERIMENTAL

A schematic diagram of the assembly (Figure 1) shows the components of the coin-cell (20 mm diameter and 3.2 mm thickness) SCs. Three SS, 18Cr9Ni from RECORD, discs pairs were used for VACNFs growth which also worked as current collectors. The diameter and thickness of the discs in the pair was different. A standard coin-cell disc 1 mm thick and 16 mm diameter was used on one side and a thin 200 μm thick and 14 mm diameter on the other side. The lower thickness of the current collector was used on one side due to the limited total thickness possible (3.2 mm) and the smaller diameter was used to prevent any short circuit due to possible separator misalignment during assembly. The 200 μm disc was cut very carefully to avoid any kind of wrinkle that would create problems for uniform VACNF growth. The discs were first cleaned using standard cleaning 1 (SC1) to remove any organic contaminants. The palladium (Pd) catalyst layer required to grow the CNFs was deposited in two ways. On one SS pair a 10 nm thick Pd catalyst film was deposited by electron beam evaporation and it was named as Cell1. On second pair the Pd catalyst was deposited in the form of nanoparticles by spin coating a polyvinylpyrrolidone/Pd (9:1) solution (details of preparation in [16]) and named as Cell2. The VACNFs were grown directly on the current collectors using the DC-PECVD method as described previously [17, 18] and conducted for 2 hours at 550^{o}C using ammonia (NH_3) and acetylene (C_2H_2) gases. The produced VACNFs were analysed by scanning electron microscopy (SEM) performed by using a JEOL JSM-6301F. The SEM images were taken at 40^{o} tilt angle enabling the measurement of the length of the VACNFs.

The coin-cells were assembled and sealed inside a glovebox under argon atmosphere (O_2 <5 ppm, H_2O <1 ppm) by using a mechanical coin-cell crimper. A VACNF electrode on a 200 μm thick current collector was put at the bottom and then 20 μL of an electrolyte of 1 M $LiPF_6$ in EC/DMC (1:1) was poured on the VACNFs using a micropipette. The separator (Celgard) was placed on the electrode followed by another 20 μL of electrolyte and a second electrode with the VACNFs facing the separator. A spring (to guarantee a good contact) was placed on the top electrode and finally the cell was assembled by putting the top cap on the spring. A reference coin-cell was made containing only SS current collectors and named as Cell3. All the measurements were made two days after assembly to allow the electrolyte to properly and equally wet the electrodes.

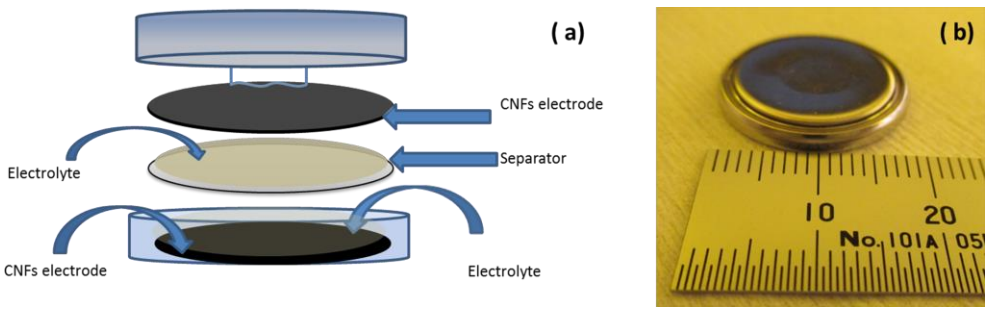

Figure 1. a) Schematic diagram of the coin-cell assembly and b) photograph of an assembled VACNF SC coin-cell.

The electrochemical performance of the coin-cells was evaluated in a two electrodes set-up by cyclic voltammetry(CV), galvanostatic charge/discharge (GCD), and electrochemical impedance spectroscopy (EIS) techniques using a Gamry Instruments Reference 3000 potentiostat equipped with the software Framework 6.33. The capacitance was measured using CV, in which the voltage at the working electrode was swept to a set potential and back to the initial voltage at a certain voltage scan rate, and the corresponding current at the working electrode was plotted vs. the voltage. The capacitance was calculated by integrating the charge and discharge curves. For an ideal SC the CV has a rectangular shape illustrating immediate change in current direction on reversing the sweep voltage. The rate capability i.e. the capacitance retention at higher voltage scan rates, was evaluated by measuring the capacitance at scan rates ranging from 20-200 mV/s. The IR drop, the energy loss or initial voltage drop due to the intrinsic resistance of electrolyte and electrode materials [19], and the cycle life were both evaluated by GCD in which the capacitor is charged to a set potential and then discharged using a constant current - here from 0 to 3.5 V and back to 0 V using a 1 A/g current density. Finally, the ESR and the capacitance behavior at different frequencies were measured by electrochemical impedance spectroscopy (EIS); a small AC potential is applied and the corresponding AC current signal is recorded – here 10 mV is applied in the frequency range 10 mHz to 1 MHz under open circuit voltage (OCV) conditions.

3. RESULTS AND DISCUSSION

The SEM micrographs of VACNFs grown using Pd catalyst both in film form and nanoparticles form (Figure 2) respectively, show the resulting VACNFs to be quite similar in length and density indicating that the Pd nanoparticles are coated uniformly on the current collector similar to the evaporated film. As the nanoparticle process is cheaper, faster and easier to perform which is practically an important observation. The lengths of the VACNFs and the capacitances of the coin-cells are provided in Table 1.

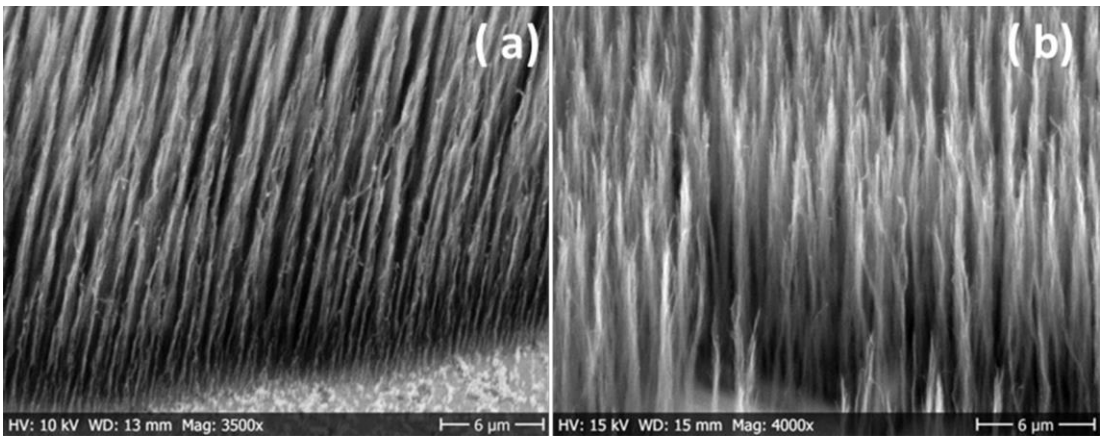

Figure 2. a) CNFs grown at 10 nm thick palladium catalyst film b) CNFs grown on palladium nanoparticles.

The CVs of Cell1 and Cell2 (Table 1 and Figure 3a) are fairly rectangular showing a typical SC behavior with capacitances of 5-5.6 mF (20 mV s^{-1}), which is 15 times higher than reference coin-cell without any CNFs. At a higher scan rate, 200 mV s^{-1}, 48% of the initial capacitance is retained for Cell1 and 70% for Cell2. Reducing the scan rate to 4 mV s^{-1} results in 10 mF (Cell1) and 8 mF (Cell2), ascribed to the existence of the micropores in the electrodes accessible only at lower scan rates due to diffusion resistance.

The GCD measurements (Figure 4a) to quantify the IR drops show nearly isosceles triangular shapes for both Cell1 and Cell2 demonstrating a smooth charge-discharge behavior of the VACNF based coin-cell SCs. However, the two cells differ in terms of IR drop represented by the vertical line in discharge curve. The IR drops for Cell1 (59 mV) and Cell2 (29 mV) are very small indicating a low internal resistance which will result in high power delivery from the cells because of the proportionality of power to the discharge voltage [20].

The cycle life of both cells after 2000 charge/discharge cycles (Figure 4b) shows that more than 80% of the capacitance is retained for Cell2 indicating an acceptably long cycle life – seen in the light of this proof-of-concept study with highly non-optimized conditions. However, the capacitance increases for Cell1 with the number of cycles unlike for Cell2, a rather odd behavior which possibly is due to a slower penetration of the electrolyte into the micropores and hence with time accessing more of the surface area of the electrode. This is supported by the higher capacitance of Cell1 at the slower scan rate (above).

Table 1. Lengths of VACNFs and capacitance of coin-cells**.**

	Catalyst deposition	VACNFs Length	Capacitance (mF)
Cell1	Film	21.1	5.6
Cell2	Nanoparticles	21.5	5
Cell3	None	No CNFs	0.32

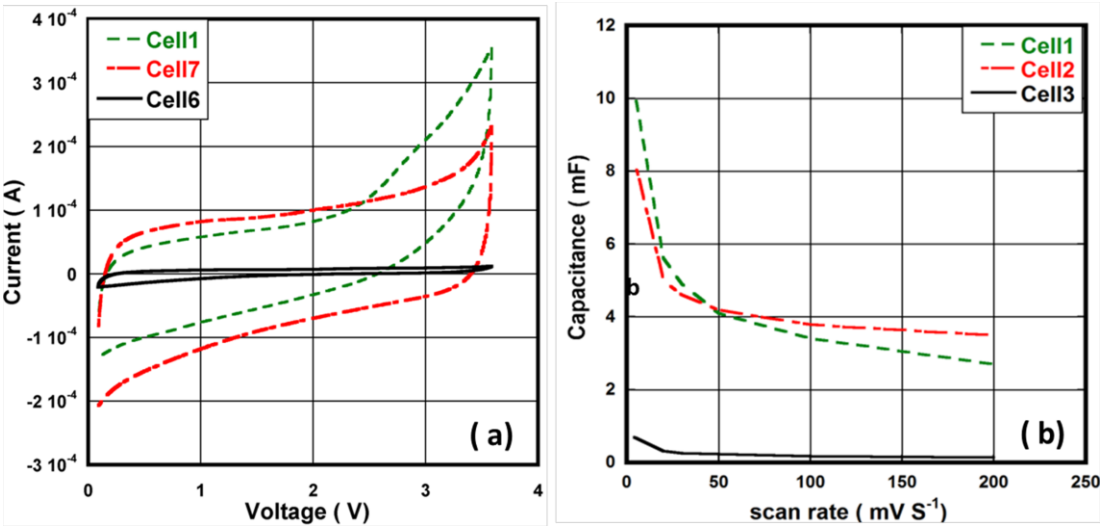

Figure 3. a) Cyclic voltammograms of Cell1, Cell2 and Cell3 at 20 mV/s b) capacitance versus scan rate.

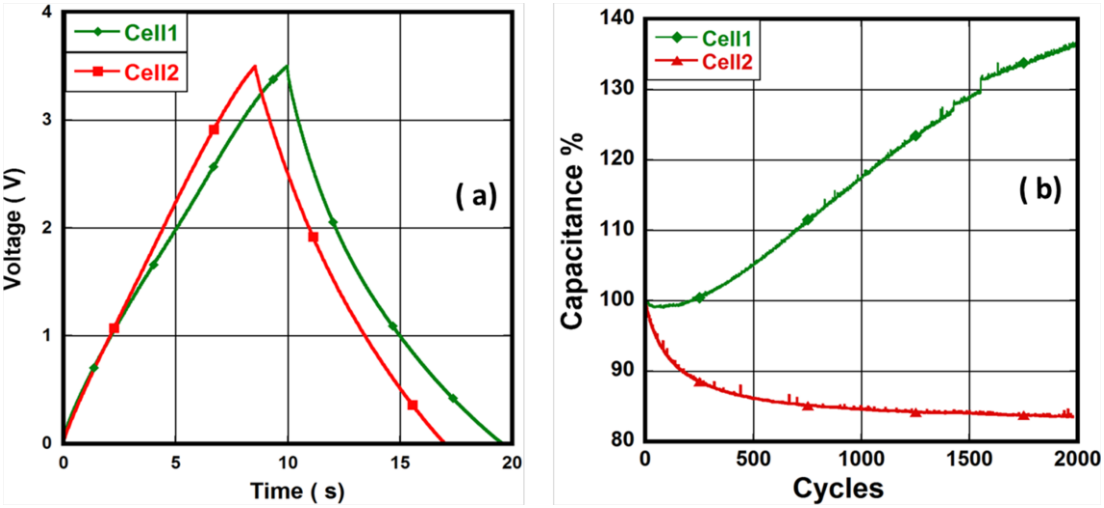

Figure 4. a) Galvanostatic charge/discharge and b) percentage capacitance as a function of cycling.

The results of the EIS measurements to quantify the ESR and the capacitive performance are shown in Figure 5. The impedance phase angles of both capacitors at different frequencies are shown in Figure 5a. The -45^{o} phase angle represents equal magnitudes of resistance and reactance of the SCs and the corresponding frequency, called characteristic frequency, is used for comparison purposes and it also relates to the switching speed of capacitor [21, 22]. However, a -90^{o} phase angle represents the ideal capacitor behavior. Here the phase angle at 1 Hz is 80^{o} and 85^{o} for Cell1 and Cell2, respectively, suggesting that the SCs behave close to an ideal capacitor [23], and the values are higher than for commercial 1 F capacitors (NEC and Panasonic) [24]. The characteristic frequencies for Cell1 and Cell2 are considerably high, 75.6 Hz and 50 Hz, respectively, and the corresponding time constants are 13 ms and 20 ms, respectively. The time constants are fairly short and comparable to SCs based on VACNTs (21 ms) and laser-scribed graphene (19 ms) [22, 25].

The Nyquist plot of EIS contains three regions: initial intercept at x-axis at high frequency, a semi-circle at high-mid frequency, and a Warburg region with -45^{o} slope and a vertical line at the low frequency [26]. From Figure 5b and c, the x-axis intercept represents ESR. The low ESR, below 2 Ω, of both cells shows an adequate contact of VACNFs/current collector resulting from the direct growth of the VACNFs onto the current collector. The ESR values are lower than the coin-cell made by using organic electrolyte and directly grown graphene nanowalls on the current collector as electrode materials (7 Ω) [1]. The low ESR gives less power losses and better heat dissipation in the SCs, thus resulting in longer life time. The diameter of the semi-circle represents the charge transfer resistance (R_{CT}) at the electrode/electrolyte interface [10, 27] and here both cells are void of any semi-circle, demonstrating the good conductivity. However there exists a Warburg region with 45^{o} slope, which represents the diffusion resistance of the electrolyte inside the electrode pores [24]. The diffusion resistance is however very low for both Cell1 (0.1 Ω) and Cell2 (0.25 Ω) representing the short diffusion path lengths inside the pores. The capacitances values of the coin-cells are however lower but the value of ESR+ R_{CT} (2-2.3 Ω (~1.5 Ω cm^{-2})) is better (lower total resistance) than the values reported in the literature for the coin-cells, Table 2.

Table 2. Comparative analysis of capacitance of coin-cells from different work.

	Electrode Materials	**Current collector**	**Binder**	**ESR + R_{CT} (Ω)**	**Capacitance**
[1]	Graphene wall grown by PECVD at 1000 ^{o}C	stainless steel	No binder	7.2-10	53 F cm^{-3}
[9]	Activated stacked GO	On Aluminum foil	PVDF binder	14.83	104 F/g
[10]	Graphene and CNTs composites	coin-cell disc	electrodeposition	50	271.0 F/g
[11]	RGO/MWCNTs	Ni foam	In pellet form		112 F/g at
[29]	AC, Acetylene black and graphite composites	coin-cell disc	PVDF binder	1000	45 mF/cm^{2}
[30]	RGO, Acetylene black	coin-cell disc	PVDF binder		140 F/g
this work	VACNFs grown by PECVD	coin-cell disc	No binder	2.3	5-5.6 mF from the coin-cells

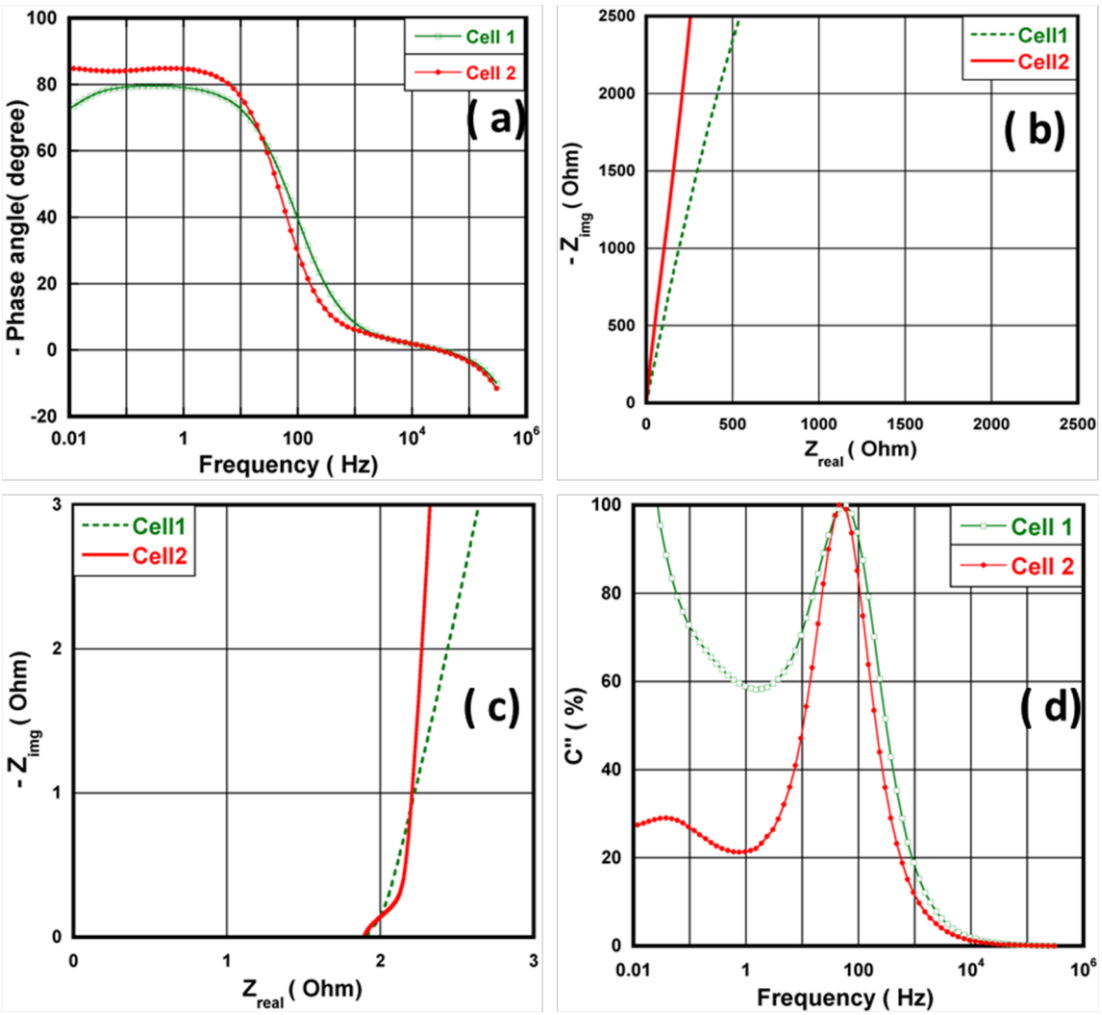

Figure 5. a) Phase angle at different frequencies b) Electrochemical impedance spectroscopy c) Zoom in d) Imaginary part of capacitance vs frequency.

The lower ESR value has an adverse effect on the power rates possible and here the low ESR for the cells assures high power delivery from the coin-cell SCs assembled, with an areal power density of 0.84-1 W/cm^2. Finally, the vertical line in the low frequency region shows the ideal capacitive behavior due to complete ion diffusion at the electrode surface and here the nearly vertical slopes for both cells indicate excellent ion diffusion. The latter is further confirmed by the fast frequency response/small relaxation time constant (τ_o), which is obtained from the imaginary part of the capacitance ($jC''(\omega)$) where $\omega=2\pi f$ [28]. The reciprocal of the frequency (f_o) obtained from the peak of C'' vs. frequency (Figure 5d) gives fairly short time constants for Cell1 (17ms) and Cell2 (25 ms), respectively, assuring fast charge/discharge possible.

4. CONCLUSIONS

Coin-cell SCs have been fabricated by growing VACNFs electrodes directly onto current collectors eliminating the need of any binder and providing excellent electrical contact. The vertical alignment facilitates the electrolyte to access the entire surface area of the CNFs and fast ion transport. The capacitances of the SCs created are up to 15 times larger than the reference SC without any CNFs. A feasibility study of these proof-of-concept SCs show a stable cycle life of 2000 charge discharge cycles and a low equivalent series resistance as verified by EIS.

ACKNOWLEDGEMENTS
This work has been performed within the mnt-era.net Carpolcap project sponsored by Vinnova, the Swedish Governmental Agency for Innovation Systems. AB, DHL, AM and PJ acknowledges the continuous support from several of Chalmers Areas of Advance: Energy, Materials Science and Transport and from the Swedish Energy Agency.

References

1. Z. Bo, Z. Wen, H. Kim, G. Lu, K. Yu and J. Chen, *Carbon*, 50 (2012) 4379.
2. Y. Rangom, X. (S). Tang and L. F. Nazar, *ACS Nano*, 9 (2015) 7248.
3. M. D. Stoller, S. Park, Y. Zhu, J. An and R. S. Ruoff, *Nano Lett*., 8 (2008) 3498.
4. H. Staaf, A. M. Saleem, G. Göransson, P. Lundgren and P. Enoksson, Carbon nanotubes as electrode for supercapacitors, 2nd International Conference on Materials for Energy, Karlsruhe, Germany, 2013.
5. T. Chen and L. Dai, *Mater. Today*, 16, 7/8(2013) 272.
6. V. Kuzmenko, A. M. Saleem, A. Bhaskar, H. Staaf, V. Desmaris and P. Enoksson, "Hierarchical cellulose-derived carbon nanocomposites for electrostatic energy storage, PowerMEMS2015, Boston, USA 2015.
7. A. M. Saleem, V. Desmaris and P. Enoksson, *J Nanomater*, 2016 (2016) 1537269.
8. M.-K. Seo and S.-J. Park, *Mater. Sci. Eng*., B, 164 (2009) 106.
9. K. Lee, D. Kim, Y. Yoon, J. Yang, H.-G. Yun, I.-K. You and H. Lee, *RSC Adv.*, 5 (2015) 60914.
10. Q. Cheng, J. Tang, N. Shinya and L.-C. Qin, *J. Power Sources*, 241 (2013) 423.
11. L. Zhou, D. He, H. Wu and Z. Qiu, *Adv. Mater. Res*, 1094 (2015) 222.
12. B. Kim, H. Chung and W. Kim, *Nanotechnology*, 23(2012) 155401.

13. R. M. Silva, A. C. Bastos, F. J. Oliveira, D. E. Conte, Y. Fan, N. Pinna and R. F. Silva, *J. Mater. Chem.* A, 3 (2015) 17804.
14. V. Desmaris, A. M. Saleem and S. Shafiee, *IEEE Nanotechnol. Mag*., 99 (2015) 33.
15. Y. Feng and S. L. Burkett, *J. Vac. Sci. Technol*., B, 33, 2(2015) 022004.
16. A. M. Saleem, S. Shafiee, T. Krasia-Christoforou, I. Savva, G. Göransson, V. Desmaris and P. Enoksson, *Sci. Tech. Adv. Mater*., 16 (2015) 015007.
17. V. Desmaris, A. M. Saleem, S. Shafiee, J. Berg, M. S. Kabir and A. Johansson, *IEEE 64th ECTC* (2014) 1071.
18. A. M. Saleem, G. Göransson, V. Desmaris and P. Enoksson, *Solid State Electron*, 107(2015) 15.
19. A. Khosrozadeh, M. Xing and Q. Wang, *Appl. Energy*, 153 (2015) 87.
20. L.-F. Chen, Z.-H. Huang, H.-W. Liang, H.-L. Gao and S.-H. Yu, *Adv. Funct. Mater*., 24 (2014) 5104.
21. J. R. Miller, R. A. Outlaw and B. C. Holloway, *Science*, 329(2010) 1637.
22. B. Hsia, J. Marschewski, S. Wang, J. B. In, C. Carraro, D. Poulikakos, C. P. Grigoropoulos and R. Maboudian, *Nanotechnology*, 25 (2014) 055401.
23. P. A. Basnayaka, M. K. Ram, L. Stefanakos and A. Kumar, *Graphene*, 2 (2013) 81-87.
24. A. Allagui, A. S. Elwakil, B. J. Maundy and T. J. Freeborn, *ChemElectroChem*, 3 (2016) 1.
25. M. F. El-Kady and R. B. Kaner, *Nat. Commun*., 4 (2013) 1475.
26. P. Sivaraman, R. Kushwaha, K. Shashidhara, V. Hande, A. Thakur, A. Samui and M. Khandpekar, *Electrochim. Acta.*, 55 (2010) 2451.
27. K. Wang, L. Li and T. Zhang, *Int. J. Electrochem. Sci*., 8 (2013) 6900.
28. C. Huang and P. S. Grant, *Sci. Rep*., 3 (2013) 2393.
29. M. Cowell, R.Winslow, Q. Zhang, J. Ju, J. Evans and P. Wright, *J. Phys. Conf. Ser*., 557 (2014) 012061.
30. S. Shivakumara, B. Kishore, T.R. Penki, and N. Munichandraiah, *ECS Electrochem. Lett.*, 4 (2015) A87.